AIAA 2000–2328

Status of Multidimensional Upwind Residual Distribution Schemes and Applications in Aeronautics

H. Deconinck and K. Sermeus
von Karman Institute for Fluid Dynamics (VKI)
Waterloosesteenweg 72
1640 Sint-Genesius-Rode, Belgium

R. Abgrall
Université Bordeaux I
351 Cours de la Libération
33 405 Talence, France

Fluids 2000
19-22 June 2000/Denver, CO

Status of Multidimensional Upwind Residual Distribution Schemes and Applications in Aeronautics

H. Deconinck* and K. Sermeus†
von Karman Institute for Fluid Dynamics (VKI)
Waterloosesteenweg 72
1640 Sint-Genesius-Rode, Belgium

R. Abgrall‡
Université Bordeaux I
351 Cours de la Libération
33 405 Talence, France

A review is made of upwind Residual Distribution Schemes (RDS) for solving advection dominated sytems on unstructured grids composed of triangles or tetrahedra. First, the design principles of RDS are explained for a steady scalar conservation law. The relation with Roe's Flux Difference Splitting scheme and with Stabilised Finite Element methods is clarified. Extension to the system of compressible flow equations is described next, and illustrated with 2D and 3D computational results in transonic and supersonic aerodynamics. More recent developments are briefly touched, such as new monotone blending schemes, an entropy fix for removing expansion shocks and consistency for the weak solution via adaptive quadrature. Finally, preliminar developments for time-accurate solutions of unsteady equations are briefly summarized.

Introduction

Present day numerical methods for the solution of advection dominated systems can be split into two main approaches, which both involve a stabilisation mechanism for the discretisation of the convective terms.

Finite Volume methods

A first class consists of the Finite Volume methods, which are obtained from a direct discretisation of the system written in integral form. In its most simple setting the steps involved are the following, for a given system of conservation laws in integral form:

- Decompose the domain in non-overlapping cells (Finite Volumes), over which the discrete solution is defined by its cell average.
- Evaluate the numerical fluxes through the boundaries of the Finite Volume. This numerical flux is computed by means of a numerical flux function, which has as arguments the two solution states at the interface, either given by the cell average itself or by a suitable reconstruction including also the neighboring cell averages.
- Use the computed flux balance for each finite volume to evolve the cell averages in time by means of a suitable time integration scheme.

The hallmark of Finite Volume methods is the close relation to the physics of the underlying conservation law, aiming to mimic as much as possible the important properties of the weak solution. For example, expressing the integral conservation laws over discrete cells ensures in a natural way discrete conservation and hence consistency with the jump relations over shocks. Another example is the stabilisation of the convective fluxes. In its most simple way this is achieved by artificial dissipation terms mimicking the viscous terms omitted from the original system[1]. Nonlinear dissipation terms (TVD, LED), are based on recovering monotonicity properties or maximum principles which hold for the conservation law. In its most sophisticated form the nonlinear physics of the conservation law is included by applying a flux function derived from the solution of the 1D Riemann problem associated with the two adjacent states[2–4]. When applied to a regular mesh of quadrilaterals this in fact corresponds to a dimension by dimension generalisation of first order upwind schemes along the curvilinear coordinates of the mesh. Higher or-

*Professor, Department of Aeronautics and Aerospace, Member AIAA.
†Ph.D. candidate, Department of Aeronautics and Aerospace, Student Member AIAA.
‡Professor, Applied Mathematics Department, Member AIAA.

der schemes can be defined by piecewise linear (or quadratic) reconstruction of the states defining the Riemann problem at the interface. Monotonicity is preserved by limiting the fluxes back to first order upwind, based on positivity requirements (LED)[5,6].
In a Finite Element setting, this approach has been generalized to the so called Discontinuous Galerkin methods[7], in which the solution in the different finite volumes is approximated by polynomials of a given maximum degree. Typical for both Finite Volume and Discontinuous Galerkin Methods is the discontinuous representation of the solution across the boundaries of the elements, and the use of flux functions to extract the flux over the boundary from the adjacent states.

Finite Element methods

A second approach follows the more classical "mathematical" framework of the Finite Element method, in which the solution is approximated with continuous functions belonging to discrete Finite Element spaces defined over the domain. The simplest example and also the choice considered in this paper is the space of linear polynomials defined over the triangles (tetrahedra in 3D) in a triangulation covering the domain, where the degrees of freedom are the solution variables defined at the vertices (P1 Finite Elements).
In this framework, the stabilisation is introduced by modifying the test function space, leading to the Petrov-Galerkin Finite Element methods. The original approach for scalar advection uses test functions which increase the weight of the upstream elements in the stencil of a given node, giving the Streamline Upwind Petrov-Galerkin (SUPG) method[8]. Subsequent generalisations are based on a Least Squares stabilisation (Galerkin Least Squares or GLS)[9].
The weak point of Stabilised Finite Element methods is the tuning of the (necessarily nonlinear) dissipation such that monotone discontinuity capturing is obtained over a small number of cells. An optimal tuning requires an eigenvector decomposition of the convective-flux Jacobians, which is obtained by the use of Riemann solvers and flux limiting in the case of Finite Volume methods. At the same time the Finite Element approach has some inherent advantages over the piecewise discontinuous model used in Finite Volume methods:

- no sophisticated reconstruction procedure is needed, second order accuracy is achieved on the compact stencil of nearest neigbours,
- the method is inherently multidimensional: for scalar advection artificial diffusion is introduced along the streamline (Streamline Diffusion),
- strong emphasis is put on consistency of the dissipation terms: they are constructed such that they vanish if the exact solution belongs to the discrete finite element space (residual property),
- strong mathematical foundations are available, allowing e.g. the perspective of superior error estimators needed for solution adaptive grid computations.

Residual Distribution Schemes

The multidimensional upwind residual distribution schemes which are the subject of this review have been developed on ideas borrowed from both the finite volume and finite element approaches discussed above, and have become nowadays an attractive alternative to either one[10]. The initial motivation for their development was a discontent about some drawbacks of the state-of-the-art finite volume solvers based on 1D approximate Riemann solvers, namely:

- For scalar advection the piecewise constant reconstruction (e.g. on a regular grid) boils down to a dimension by dimension generalisation of first order upwinding. This is well known to be the most diffusive first order scheme, whereas much less diffusive first order schemes exist, such as the Streamline Upwind scheme of Rice and Schnipke[11] or the Skew Upstream differencing schemes proposed by Raithby[12].
- 1D Riemann solvers do not capture the real multidimensional flow physics such as the preservation of entropy and total enthalpy along the streamline in smooth steady flow.
- Higher order schemes based on polynomial reconstruction use wide stencils.

The question whether it is possible to extend the "physics" built into Finite Volume methods to multiple space dimensions has also been investigated in a Finite Volume context by numerous authors[13–15], however with very modest success: it turns out that it is very difficult to avoid the bias of the normal direction when splitting the flux on a cell face in its upwind contributions. To introduce multidimensionality it seems necessary to split instead the complete flux balance over a cell (i.e. the cell residual) in its multidimensional components describing e.g. propagation of characteristic information along the streamlines or the Mach lines in supersonic flow (remark that in 1D, flux difference splitting indeed boils down to a flux balance splitting over a one-dimensional cell). It turns out that the class of Residual Distribution Schemes is a good candidate framework for such a splitting, while at the same time allowing to make the link with Petrov-Galerkin Finite Element methods. Indeed, already in 1981 R.-H. Ni proposed a Lax-Wendroff Residual Distribution scheme[16] which was further developed by Morton and coworkers[17] and has strong similarities with the Finite Element SUPG scheme on bilinear quadrilaterals. Around the same time, P.L. Roe[18] proposed a Residual Distribution framework in an upwind context under the name of fluctuation splitting schemes, starting from a reinterpretation of Roe's flux difference splitting Finite Volume scheme. This approach has been generalised in 2D in 1986[19] and is at the basis of the present multidimensional upwind schemes discussed in this paper. The close links between Residual Distribution Schemes and Petrov-Galerkin Finite Element schemes have not been emphasized in the past and even overlooked, but we believe that it is important for its future development, for example in the context of time dependent problems and error estimation.

As mentioned before, the starting point for the development of these schemes by Roe was a reinterpretation of 1D finite volume schemes based on the concept of fluctuation[18]. For the scalar conservation law with source term q

$$\frac{\partial u}{\partial t} + \frac{\partial f(u)}{\partial x} = q$$

and quasilinear form

$$\frac{\partial u}{\partial t} + a\frac{\partial u}{\partial x} = q,$$

the standard upwind finite volume scheme reads:

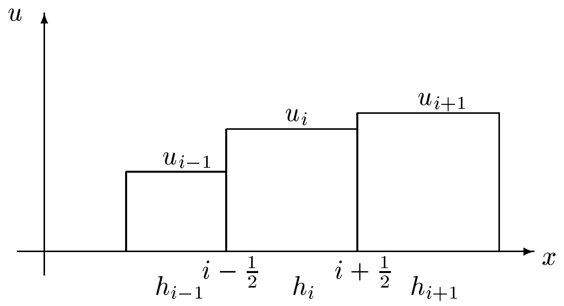

$$h_i\frac{du_i}{dt} + (f_{i+\frac{1}{2}} - f_{i-\frac{1}{2}}) = q_i h_i, \tag{1}$$

where for Roe's scheme the interface fluxes $f_{i\pm\frac{1}{2}}$ are evaluated using the numerical flux function

$$f_{i+\frac{1}{2}} = \frac{f_i + f_{i+1}}{2} - \frac{\text{sgn}(a_{i+\frac{1}{2}})}{2}(f_{i+1} - f_i).$$

If the cell averaged speed $a_{i+\frac{1}{2}}$ is computed using Roe's conservative linearisation $f_{i+1} - f_i = a_{i+\frac{1}{2}}(u_{i+1} - u_i)$, one finally obtains the following first order discretisation at steady state:

$$a^+_{i-\frac{1}{2}}(u^n_i - u^n_{i-1}) + a^-_{i+\frac{1}{2}}(u^n_{i+1} - u^n_i) = q_i h_i \tag{2}$$

where

$$a^+ = max(0, a) \qquad \text{and} \qquad a^- = min(0, a) \tag{3}$$

Consider now the interpretation of the above Roe scheme using the Residual Distribution approach:

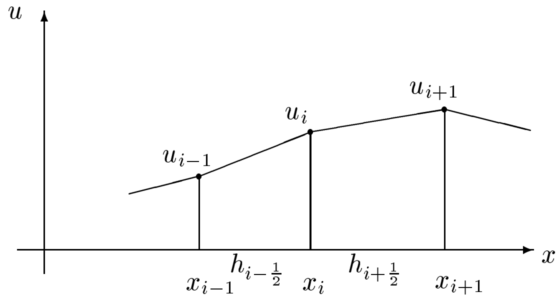

Using the continuous piecewise linear Finite Element data representation (P1 elements) rather than the discontinuous cell-wise reconstruction of finite volume methods, the cell residual is computed first as

$$\phi^{i+\frac{1}{2}} = \int_{x_i}^{x_{i+1}} (f^h_x - q^h)dx \equiv f_{i+1} - f_i - \frac{q_i + q_{i+1}}{2} h_{i+\frac{1}{2}} \tag{4}$$

where the source term has been integrated using the trapezium rule. The nodal equation for node i is then formed by distributing the cell residual to the two nodes of the cell. Gathering the contributions of the two elements at node i one obtains for the steady state equation:

$$\beta_i^{i-\frac{1}{2}}\phi^{i-\frac{1}{2}} + \beta_i^{i+\frac{1}{2}}\phi^{i+\frac{1}{2}} = 0 \tag{5}$$

where the distribution coefficients β sum to one for a given cell:

$$\beta_i^{i+\frac{1}{2}} + \beta_{i+1}^{i+\frac{1}{2}} = 1 \tag{6}$$

Clearly, the first order Roe upwind discretisation of the advection term is obtained by distributing the residual only to the downstream node,

$$\beta_i^{i+\frac{1}{2}} = \frac{a^-_{i+\frac{1}{2}}}{a_{i+\frac{1}{2}}} \qquad \beta_{i+1}^{i+\frac{1}{2}} = \frac{a^+_{i+\frac{1}{2}}}{a_{i+\frac{1}{2}}}, \tag{7}$$

giving for the steady state equation (5):

$$a^+_{i-\frac{1}{2}}(u^n_i - u^n_{i-1}) + a^-_{i+\frac{1}{2}}(u^n_{i+1} - u^n_i) = \frac{a^+_{i-\frac{1}{2}}}{a_{i-\frac{1}{2}}}\frac{q_{i-1}+q_i}{2}\,h_{i-\frac{1}{2}} + \frac{a^-_{i+\frac{1}{2}}}{a_{i+\frac{1}{2}}}\frac{q_i+q_{i+1}}{2}\,h_{i+\frac{1}{2}} \tag{8}$$

Comparing equations (2) and (8), we observe an important difference between the source term discretisation of the two approaches: While in absence of the source term the two discretisations become identical (being in fact both second order), the Residual Distribution method remains second order in the steady for a non-zero source term, even with a "first order" Roe scheme, while the Finite Volume scheme becomes first order in space. This result even holds for an arbitrary non-uniform mesh and stems from the fact that for *bounded* distribution coefficients the nodal equation is formed as a linear combination of cell residuals including the source term, which vanish each individually up to third order for smooth solutions of the conservation law with source term, precisely as in Finite Element methods, where this property is called the residual property.

The upwind residual distribution interpretation can be carried over to two and three dimensions, provided the residual is now the flux balance over a simplex (triangle/tetrahedron), supplemented with the source term, to which is associated a continuous piecewise linear data representation. Because the elementary discretisation unit is an element rather than an edge or face for the finite volume method, the multidimensionality of the problem can genuinely be taken into account: in 2D, the fluctuation can be distributed to the *three vertices* of the triangle rather than to the two neighbouring cells of an edge. Moreover, by distributing the residual only to the downstream vertices of the triangle or tetrahedron (with respect to an averaged advection velocity vector), truely multidimensional upwinding can be introduced.

Based on these ideas, schemes were constructed in 2D and 3D, which combine a number of attractive features:

- a first order scheme with much lower cross-diffusion than its finite volume counterpart, due to the genuinely multidimensional upwinding it incorporates, very similar to the Streamline Upwind scheme[11],
- a positivity (or LED) property which ensures the satisfaction of a discrete maximum principle and consequently the absence of spurious oscillations,
- schemes with (almost) second order accuracy on compact stencils.

In addition, the compact discretisation stencil (a property shared with the Petrov Galerkin approach), allows for the development of efficient implicit iterative solution strategies[20] and for an easy parallelisation[21,22].

The paper starts with a discussion of upwind residual distribution schemes for steady and unsteady scalar conservation laws. Next their application to non-linear systems, specifically the compressible flow equations, is presented. Finally, the paper concludes with a few illustrative computational examples.

Residual Distribution schemes for a scalar conservation law

Steady scalar conservation law

The residual distribution schemes (RDS) have been designed for an optimal discretisation of the steady state conservation law

$$\vec{\nabla} \cdot \vec{f} = 0 \qquad \text{or} \qquad \vec{\lambda} \cdot \nabla u = 0 \tag{9}$$

on P1 finite element meshes, i.e. triangular (resp. tetrahedral) meshes with a piecewise linear solution representation u^h. We first define the cell residual or fluctuation over an element T as the integral over this element of the differential operator, i.e.

$$\phi^T = \int_T \vec{\nabla} \vec{f}^h \, d\Omega \equiv \Omega_T \vec{\bar{\lambda}} \cdot \vec{\nabla} u^h. \tag{10}$$

Since ∇u^h is constant because of the P1 element, an exact equivalence between the conservative form and the quasilinear form of the residual is found if the cell-averaged advection speed $\vec{\bar{\lambda}}$ is computed by the exact integration of

$$\vec{\bar{\lambda}} = \frac{1}{\Omega_T} \int_T \vec{\lambda}(u^h) \, d\Omega. \tag{11}$$

This definition is called a conservative Roe-linearisation and allows to work with the quasilinear expression while maintaining conservation. One finally obtains for the cell residual

$$\phi^T = \sum_i k_i u_i, \tag{12}$$

where $k_i = \frac{1}{d} \, \vec{\bar{\lambda}} \cdot \vec{n}_i$ is called the inflow parameter, $\vec{n}_i$ being the scaled inward normal of the edge opposite to node i (see Fig. 1) and d the number of spatial dimensions. The Residual Distribution method consists in distributing fractions of ϕ^T to the vertices of the element. The resulting discrete equations therefore express that the nodal residuals R_i, sum of all contributions from neighbouring elements, vanish, i.e.

$$R_i = \sum_T \phi_i^T = \sum_T \beta_i^T \phi^T = 0 \tag{13}$$

in which β_i^T are the distribution coefficients and ϕ_i^T denotes the part of the residual ϕ^T of element T which is sent to node i. On each element T, the distribution coefficients must sum up to one for consistency and conservativity. In[23] it is shown that under reasonable assumptions on the ϕ_i^Ts (continuity, convergence of f^h towards f, continuity of f^h on the edges of T) and the classical assumption of the Lax-Wendroff theorem, the numerical solution converges to a weak solution of (9).

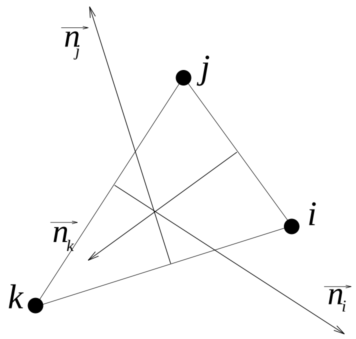

Fig. 1 Triangular element with scaled inward normals.

Table 1 Residual distribution schemes

Scheme	β_i^T	type	$\mathcal{U}$	$\mathcal{P}$	$\mathcal{LP}$
N	$k_i^+(\phi^T \sum_j k_j^-)^{-1} \sum_j k_j^-(u_i - u_j)$	linear	$\surd$	$\surd$	
LDA	$(\sum_j k_j^+)^{-1} k_i^+$	linear	$\surd$		$\surd$
SUPG	$\frac{1}{d+1} + \tau \frac{k_i}{\Omega_T}, \quad \tau = \frac{1}{2} \frac{h}{\Vert\vec{\lambda}\Vert}$	linear			$\surd$
L-W	$\frac{1}{d+1} + \frac{k_i}{\sum_j \vert k_j \vert}$	linear			$\surd$
PSI	$\max(0, \beta_i^N) / \sum_i \max(0, \beta_i^N)$	non-linear	$\surd$	$\surd$	$\surd$

Design principles

Different schemes, corresponding to different ways of computing the distribution coefficients, have been designed to satisfy several properties making them optimal:

$\mathcal{U}$**:** Upwind character. No fraction of the element residual is sent to upstream nodes:
$\phi_i^T = 0$ when $k_i \leq 0$.

$\mathcal{P}$**:** Positivity. The scheme does not create local extrema or, if we write the contribution of element T to node i as $\phi_i^T = \sum_j c_{ij} u_j$, we impose: $c_{ij} \leq 0 \ \forall j \neq i$.

$\mathcal{LP}$**:** Linearity preservation. The distribution coefficients β_i^T remain bounded as $\phi^T \rightarrow 0$ which is equivalent to zero cross-diffusion (second order accuracy) on a regular mesh.
A more general way of getting second order accuracy at steady state is to require that the residual ϕ_i^T satisfies the property[24]

$$\phi_i^T(u^h) = O(h^3) \tag{14}$$

for an exact solution (9) assumed to be regular and u^h its piecewise linear interpolation on the mesh. Indeed, because of the accuracy properties of the piecewise linear interpolation on a regular mesh, it is easy to see that the total residual evaluated for u^h satisfies $\phi^T = O(h^3)$, so that the boundedness of $\beta_i^T = \frac{\phi_i^T}{\phi^T}$ implies (14). The advantage of (14) over asking the boundedness of the β_i^Ts is that it is easier to handle for systems.

$\mathcal{C}$**:** Continuity. The distribution coefficients must be continuous functions of both the advection and the solution-gradient directions.

Scalar advection schemes

Several schemes satisfying some or all of these design criteria have been developed both in 2D and 3D. A complete summary is given in[25] and is not repeated here. Some schemes are summarized in Table 1 (formulas valid both for 2D and 3D), where $k_i^+ = \max(0, k_i)$, $k_i^- = \min(0, k_i)$. The N-scheme is a linear monotone ($\mathcal{P}$) first order upwind scheme, the LDA scheme a second order ($\mathcal{LP}$) linear upwind scheme, and the PSI scheme a nonlinear second order ($\mathcal{LP}$) *and* monotone ($\mathcal{P}$) upwind scheme obtained by applying a limiter to the distribution coefficients of the N-scheme, following a technique proposed by Sidilkover[26,27]. Note that as a result of a generalisation of Godunov's theorem, only non-linear schemes can satisfy both the $\mathcal{P}$ and $\mathcal{LP}$ properties.

Nonlinear blending schemes

An interesting recent development in this respect[28] is the proposal of new nonlinear blending schemes resulting from a combination of the first order monotone N-scheme and the second order non-monotone LDA scheme: On a triangle T (the superscript T will be omitted), the residual distributed to node i is defined as

$$\phi_i = l \ \phi_i^N + (1 - l) \ \phi_i^{LDA} \tag{15}$$

where $0 \leq l \leq 1$ is a nonlinear blending coefficient. We look for l such that the scheme is monotone ($\mathcal{P}$) and $\mathcal{LP}$. A heuristic definition which is $\mathcal{LP}$ and causes a bias to the N-scheme in regions where the cell residual is large (typically in shocks), is given by

$$l = \frac{|\phi|}{\sum_i |\phi_i^N|} \tag{16}$$

A rigorous analysis imposing both positivity and linearity preservation is performed in[29]. It turns out that the solution is non unique, but that the most natural choice gives back the PSI-scheme known since 1992. In this case l is obtained as follows (assuming the 2D case of triangles):

One target case : Two of the 3 inflow parameters k_j are negative and one is positive. As for any scheme satisfying $\mathcal{U}$, the residual is send to the unique downstream node and both N-scheme and LDA scheme give the same result, hence one can take $l = 1$,

Two target case : One of the 3 inflow parameters k_j is negative and two are positive. Assume that $k_i, k_j > 0$ and $k_k \leq 0$. We denote by

$$r_i = \frac{\phi_i^{LDA}}{\phi_i^N} \quad r_j = \frac{\phi_j^{LDA}}{\phi_j^N}.$$

we find that $l = \max(\varphi(r_i), \varphi(r_j))$ where

$$\varphi(x) = \begin{cases} \dfrac{x}{1-x} & \text{if } x < 0 \\ 0 & \text{else} \end{cases} \tag{17}$$

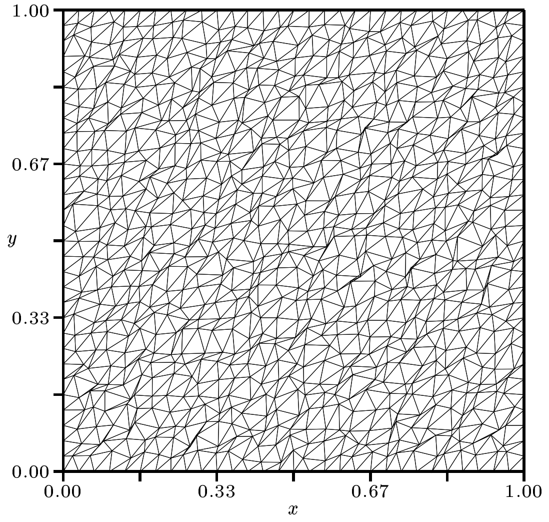

Fig. 2 Distorted mesh for the oblique shock problem.

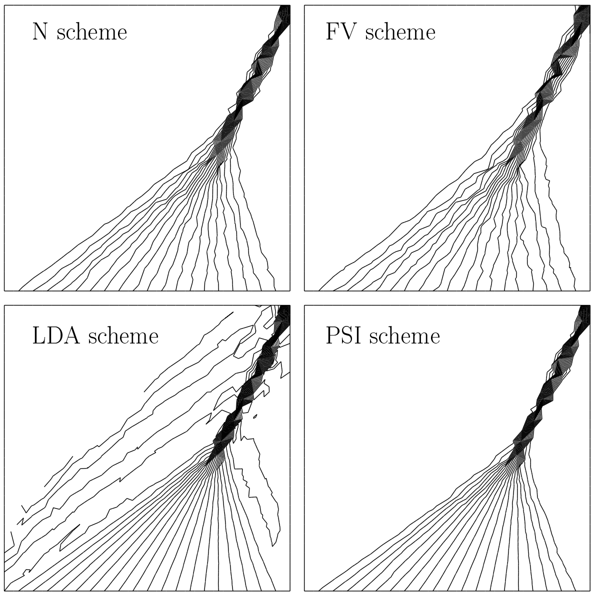

Fig. 3 Oblique shock test case on distorted mesh: solution for finite volume, N, LDA and PSI schemes.

Another choice, leading to a different scheme, would be defined with $l = \max(\varphi(|r_i|), \varphi(|r_j|))$ In conclusion, for scalar advection no improvements over the PSI scheme are to be expected. However, for systems of equations the blending approach provides an alternative to construct nonlinear monotone schemes, since system generalisations of the original PSI scheme have turned out to be quite difficult.

Example computation

The testcase is a 2D variant of the inviscid Burgers' equation, with flux and quasilinear form given by:

$$\vec{f}(u) = \begin{pmatrix} u^2/2 \\ u \end{pmatrix} \qquad u\frac{\partial u}{\partial x} + \frac{\partial u}{\partial y} = 0. \tag{18}$$

A severely distorted 31×31 mesh (Figure 2) is used to compute the solution of an oblique shock problem on the domain $(x, y) \in [0, 1]^2$, with boundary conditions: $u(x, 0) = 1.5 - 2x$, $u(x = 0, y) = 1.5$, $u(x = 1, y) = -0.5$. The exact solution varies linearly up to the point where the characteristics merge (the intersection point, determined by the intersection of the limiting characteristics, is located at $x = \frac{3}{4}$, $y = \frac{1}{2}$), forming a discontinuity which lies oblique to the mesh.

The SUPG scheme (even with nonlinear shock capturing dissipation) is unstable on this mesh, probably because of the extreme angles present in some elements which are known to destabilize the Galerkin method. The solutions of the most robust schemes (N, first order upwind FV, LDA and PSI) are plotted in Figure 3. The failure of the linear positive schemes to represent linearly varying solutions is pronounced, especially in the case of the first order upwind finite volume scheme. On the other hand, the compression fan is well defined in the case of the linearity preserving schemes (LDA and PSI), with monotone shock-capturing in the case of the PSI scheme.

Finite element interpretation

Although the starting point was a reinterpretation of finite volume schemes using the concept of fluctuation, RDS schemes have in fact more common ground with finite element methods: They can be viewed as a particular class of Petrov-Galerkin finite element schemes where the test functions are carefully designed to satisfy some or all of the above properties. Indeed, denoting ω_i^T the weighting function associated to node i of element T, the Petrov-Galerkin discretisation of the advection equation (9) can be written as

$$\sum_T \int_T \omega_i^T \vec{\lambda} \cdot \vec{\nabla} u^h \, d\Omega = 0. \tag{19}$$

Now, from the definition of ϕ^T and from the linear approximation of u^h over T, assuming a constant advection vector $\vec{\lambda}$, $\vec{\lambda} \cdot \nabla u$ is constant over T and equal to ϕ^T / Ω_T, where Ω_T is the surface of the triangle T (volume of the tetrahedron T in 3D). Hence, the previous equation becomes

$$\sum_T \int_T \omega_i^T d\Omega \, \frac{\phi^T}{\Omega_T} = 0. \tag{20}$$

For the Petrov-Galerkin discretisation to be identical to the residual distribution discretisation (13), the weighting functions ω_i^T should satisfy the following relation :

$$\int_T \omega_i^T d\Omega = \Omega_T \beta_i^T. \tag{21}$$

This equation is not sufficient to uniquely associate a weighting function ω_i^T to a residual distribution coefficient β_i^T unless the functional form of the weighting function is prescribed and depends on a single parameter. Prescribing the weighting function to be the sum of the finite element shape function φ_i and a piecewise constant contribution similar to SUPG weighting functions[30], i. e. $\omega_i^T = \varphi_i + \alpha_i^T \gamma^T$, where α_i^T is the upwind bias coefficient and γ^T is the piecewise constant function equal to 1 on element T and 0 elsewhere, the equivalence condition (21) yields

$$\frac{1}{\Omega_T}\int_T (\varphi_i + \alpha_i^T \gamma^T)\, d\Omega = \beta_i^T, \tag{22}$$

giving

$$\beta_i^T = \frac{1}{d+1} + \alpha_i^T, \tag{23}$$

where $d+1$ is the number of vertices of the simplex (3 in 2D, 4 in 3D). Hence, one obtains an equivalence for the following choice of the Petrov-Galerkin test function:

$$\omega_i^T = \varphi_i + (\beta_i^T - \frac{1}{d})\gamma^T. \tag{24}$$

Clearly, for equidistribution of the residual over all vertices of the simplex, $\beta_i^T = 1/(d+1)$, the residual distribution scheme reduces to a pure Galerkin finite element method (unstable for advection). Note also that the first order N-scheme cannot be obtained from a Petrov-Galerkin approach since the distribution coefficients β and hence the corresponding test functions are unbounded for vanishing cell residual, due to the fact that the N-scheme is not $\mathcal{LP}$.

Extension to unsteady scalar advection

The Residual Distribution approach has originally been developed for steady conservation laws. Recently, the work on extensions to unsteady equations has started. Consider the unsteady scalar advection equation

$$\frac{\partial u}{\partial t} + \vec{\lambda}\cdot\vec{\nabla} u = 0, \tag{25}$$

Petrov-Galerkin Flux Corrected Transport (PG-FCT)

A first approach starts from a consistent Petrov Galerkin formulation where the Petrov-Galerkin test functions applied to the unsteady conservation law are defined according to the distribution scheme following equation (24). The general semi-discretization of equation (25) is then:

$$\sum_T \sum_j m_{ij}^T \frac{du_j}{dt} + \sum_T \beta_i^T \phi^T = 0, \tag{26}$$

where in the first term on the left hand side a consistent mass matrix appears, given by[31] :

$$m_{ij}^T = \int\int_{\Omega_T} \omega_i \varphi_j d\Omega =$$

$$\frac{\Omega_T}{3}\begin{bmatrix} \frac{1}{2}+\beta_1^T-\frac{1}{3} & \frac{1}{4}+\beta_1^T-\frac{1}{3} & \frac{1}{4}+\beta_1^T-\frac{1}{3} \\ \frac{1}{4}+\beta_2^T-\frac{1}{3} & \frac{1}{2}+\beta_2^T-\frac{1}{3} & \frac{1}{4}+\beta_2^T-\frac{1}{3} \\ \frac{1}{4}+\beta_3^T-\frac{1}{3} & \frac{1}{4}+\beta_3^T-\frac{1}{3} & \frac{1}{2}+\beta_3^T-\frac{1}{3} \end{bmatrix} \tag{27}$$

For steady state computations this mass matrix is usually lumped by summing all elements on a given column to the diagonal, giving the so called inconsistent Galerkin lumped mass matrix:

$$m_{ij}^{L,inc,T} = \frac{\Omega_T}{3}\,\mathbf{I} \tag{28}$$

Due to the consistent mass matrix, the unsteady scheme is implicit in time. For the time integration, any second order scheme can be used. In the present work, Crank-Nicholson time-stepping has been applied[32] :

$$\left[\frac{\mathbf{M}}{\Delta t} + \frac{\mathbf{J}}{2}\right]\Delta U^n = -R^n, \tag{29}$$

where $\mathbf{J}$ is the jacobian of the nodal residual R.

The approach is second order in time, but has some severe drawbacks: first, the N-scheme cannot be used in this framework, since the distribution coefficients are unbounded for vanishing cell residual. Second, the mass matrix is not guaranteed positive definite, such that the scheme loses its positivity properties, even if e.g. the monotone PSI scheme has been chosen as the underlying RDS scheme.

In[32, 33] a cure was proposed based on the well-known Flux Corrected Transport (FCT) approach[34], by combining a low order method (N-scheme or PSI scheme with inconsistent lumped mass matrix), with the above high order non-monotone scheme. Although this approach works reasonably well, it is clearly unsatisfactory from the theoretical point of view. Another shortcoming is that the compactness of the stencil is lost due to the FCT limiting.

Lax-Wendroff Flux Corrected Transport (LW-FCT)

The Lax-Wendroff scheme is the unique *explicit* scheme which is second order accurate in both time and space on the compact stencil of nearest neighbours. It is given by[33, 35] :

$$u_i^{n+1} = u_i^n - \frac{\Delta t}{\Omega_i}\sum_T \beta_i^{T,LW}\phi^{T,n}, \tag{30}$$

where Ω_i is the median dual cell around node i obtained from the assembly of the lumped element mass matrices, while for the Lax-Wendroff scheme[10] :

$$\beta_i^{T,LW} = \frac{1}{3} + \frac{\Delta t}{2\Omega_T}k_i. \tag{31}$$

Again, an FCT blending with a monotone (N or PSI) scheme is necessary in order to obtain a monotone scheme in time.

Space-time Residual Distribution schemes

Another way of proceeding is to see the PDE as a whole and to define a space–time residual $\Phi_{x,t}$ for the operator

$$\frac{\partial}{\partial t} + \vec{\lambda}\cdot\vec{\nabla}.$$

To do so, we consider the space–time element $T \times [t_n, t_{n+1}]$ and approximate the solution piecewise linearly in space and time:

$$u^h(x,t) = u^n(x)\frac{t_{n+1}-t}{\Delta t} + u^{n+1}(x)\frac{t-t_n}{\Delta t}$$

where u^n (resp. u^{n+1}) stands for the piecewise linear interpolation of the data u_j^n (resp. u_{j+1}^n) at the vertices of T. The total fluctuation is

$$\Phi_{x,t} = \int_T \int_{t_n}^{t_{n+1}} \left(\frac{\partial u^h}{\partial t} + \vec{\lambda}\cdot\vec{\nabla} u^h\right) dxdt,$$

that is

$$\Phi_{x,t} = \sum_{i\in T} \Phi_i^t + \Phi^s$$

where

$$\begin{aligned} \Phi_i^t &= \frac{\Omega_T}{3}(u_i^{n+1} - u_i^n) \\ \Phi^s &= \frac{\Delta t}{2}\sum_{i\in T} k_i(u_i^{n+1} + u_i^n). \end{aligned}$$

The design principles are the same as for the steady case, namely the $\mathcal{U}$ and $\mathcal{LP}$ properties.

We first define an extension of the steady N scheme :

- for the vertices at time t^n: $\phi_{i,n}^N = 0$ for each vertex of T,
- for the vertices at time t_{n+1},

$$\begin{aligned} \phi_{i,n+1}^N = \tfrac{\Omega_T}{3}(u_i^{n+1} - u_i^n) \quad &+ \quad \tfrac{\Delta t}{2}k_i^+(u_i^{n+1} - \widetilde{u}^{n+1}) \\ &+ \quad \tfrac{\Delta t}{2}k_i^+(u_i^n - \widetilde{u}^n) \end{aligned}$$

where $\widetilde{u}^{n+1}$ and $\widetilde{u}^n$ are computed to get the (space-time) conservation,

$$\widetilde{u}^{n+1} = N\sum_{j=1}^{3} k_j^- u_j^{n+1} \qquad (32)$$

$$\widetilde{u}^{n} = N\sum_{j=1}^{3} k_j^- u_j^{n} \qquad (33)$$

and N defined as usual $N = \left(\sum_{i\in T} k_i^-\right)^{-1}$.

This scheme can be proved to be positive under the CFL condition,

$$\Delta t \leq \frac{2}{3}\frac{\Omega_T}{k_i^+} \qquad (34)$$

Next, we need to define a second order (in space and time) scheme which residuals sum up to $\Phi_{x,t}$ as for the previous scheme. A not so obvious choice is the Petrov-Galerkin scheme defined by (26)–(27).

Here, we extend the LDA scheme to space-time defining it as

$$\Phi_{i,n}^{LDA} = 0$$

$$\Phi_{i,n+1}^{LDA} = (\beta_i + \tfrac{1}{6})\phi_i^t + (\beta_i - \tfrac{1}{12})\textstyle\sum_{j\neq i}\phi_j^t + \beta_i\phi^s.$$

where, as in the steady case, $\beta_i = (\sum_j k_j^+)^{-1}k_i^+$.

To construct a second order positive scheme, one can apply the blended approach as in the steady case, here applied to the space–time fluctuations. The residuals distributed to the nodes are defined by

$$\Phi_{i,n} = 0$$

$$\Phi_{i,n+1} = l\Phi_{i,n+1}^N + (1-l)\Phi_{i,n+1}^{LDA}$$

where $l = \max(\varphi(r_i), \varphi(r_j), \varphi(r_k))$ with

$$r_i = \frac{\Phi_{i,n+1}^{LDA}}{\Phi_{i,n}^N} \quad \text{same for } j \text{ and } k$$

and φ defined by (17).

The scheme reads

$$\sum_T \left(l\phi_{i,n+1}^N + (1-l)\phi_{i,n+1}^{LDA}\right) = 0 \qquad (35)$$

The non linear system is solved by Newton iterations. We have experimentally noticed that the blending parameter defined by

$$l = \frac{|\Phi_{x,t}|}{\sum_j |\Phi_{i,n+1}^N|}$$

works very well, even though it does not satisfy the positivity requirements.

Example computation

The first testcase[35] concerns the rotation of a cylindrical hill in a circular solid body advection field centered at the origin ($\vec{\lambda} = [2\pi y, -2\pi x]$). The initial solution is defined by $u(t=0,x,y) = 1$ for $r \leq 0.25$ and $u(t=0,x,y) = 0$ for for $r \geq 0.25$, with $r = \sqrt{(x+0.5)^2 + y^2}$. Hence, after one revolution, the cylinder has to be found back in the starting position. A square diamond mesh with 80×80 meshpoints was used, and the ratio $\Delta t/\Delta x = 0.08$ was fixed. In Figure 4a and 4b, the isolines of the solution after one revolution are compared for the explicit Lax-Wendroff/PSI-FCT scheme and the implicit Cranck-Nicholson LDA/PSI-FCT scheme. In both cases PSI was selected as the low order scheme in the FCT blending. Perfect monotone results are obtained in both cases. The implicit scheme performs substantially better than the explicit scheme, however at a much higher cost.

Next, we compare results for the advection of a cosine hill, after one rotation, for a classical MUSCL scheme with Heun's time integration (2-step Runge-Kutta) and using minmod limiter (Figure 5a) with the blended space-time scheme (Figure 5b). The quasi-uniform unstructured mesh has 11382 nodes. The CFL number defined by (34) is set to 0.5. There is an evident improvement of the results.

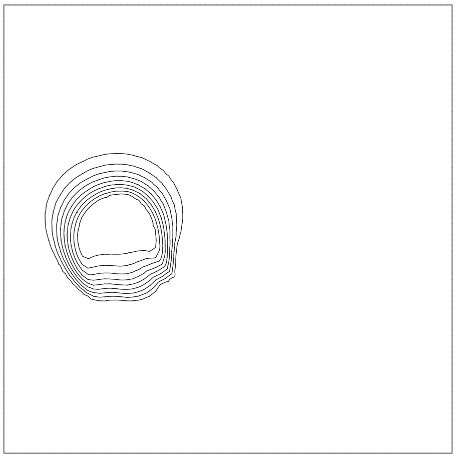

a)

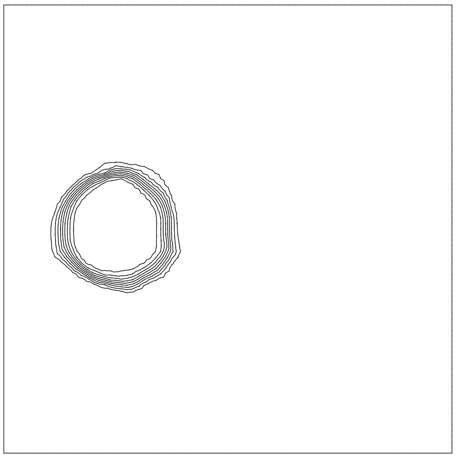

b)

Fig. 4 Solid body rotation of cylindrical profile. Solution isolines after one revolution for : a) explicit L-W/PSI-FCT scheme and b) implicit LDA/PSI-FCT scheme with Crank-Nicholson time-stepping.

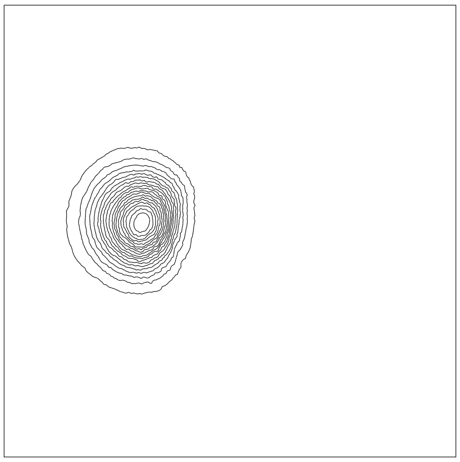

a)

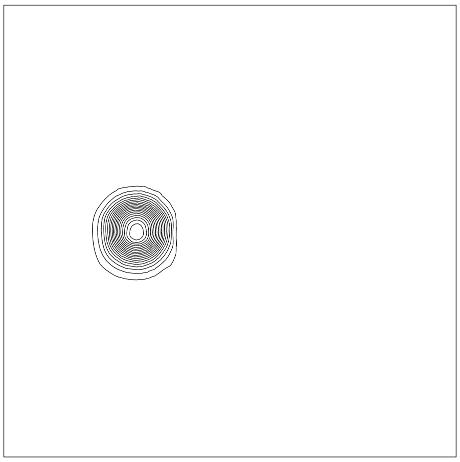

b)

Fig. 5 Solid body rotation of a cosine hill. Solution isolines after one revolution for : a) explicit MUSCL scheme (min=0., max=0.45) and b) implicit blended LDA/N space-time scheme (min=0, max=0.89).

Residual Distribution Schemes for the Compressible Flow Equations

Consider first the system of Euler equations of gasdynamics given by

$$\vec{\nabla} \cdot \vec{\mathbf{F}} = 0 \qquad \text{or} \qquad \mathbf{A}_\ell \frac{\partial \mathbf{U}}{\partial x_\ell} = 0, \tag{36}$$

where $\vec{\mathbf{F}}$ are the inviscid fluxes and $\mathbf{A}_\ell$ their Jacobians in Cartesian coordinates.

The formal extension of the Residual Distribution discretisation (13) is

$$\mathbf{R}_i = \sum_T \Phi_i^T = \sum_T \beta_i^T \Phi^T = 0 \tag{37}$$

where the cell residual Φ^T is now a vector whose dimension is the dimension of the system, while the β_i^T have become distribution *matrices*.

Roe-Struijs-Deconinck linearisation

For reasons of conservation, a quasilinear form of the cell residual is sought which generalises (10) and (11) for the system case. Such a conservative linearisation consists in finding on each triangle T an average state $\bar{\mathbf{U}}$ such that for the integral form of the residual, one has

$$\Phi^T = \oint_{\partial\Omega_T} \mathbf{F}_\ell^h n_\ell \, d\Gamma \equiv \Omega_T \underbrace{\mathbf{A}_\ell(\bar{\mathbf{U}})}_{\bar{\mathbf{A}}_\ell} \frac{\partial \mathbf{U}^h}{\partial x_\ell} \tag{38}$$

where

$$\frac{\partial \mathbf{U}^h}{\partial x_\ell} \equiv \frac{1}{\Omega_T} \oint_{\partial\Omega_T} \mathbf{U}^h n_\ell \, d\Gamma \tag{39}$$

In this way, the non-linear system of conservation laws $\vec{\nabla}\mathbf{F} = 0$ is locally approximated by the linear system

$\bar{\mathbf{A}}_\ell \partial \mathbf{U}/\partial x_\ell = 0$. Let's show that, with such a linearisation, conservation is indeed satisfied. Summing up the nodal residuals over the domain Ω, we have

$$\begin{aligned}\sum_i \mathbf{R}_i &= \sum_i \sum_T \Phi_i^T = \sum_T \underbrace{\sum_i \Phi_i^T}_{=\Omega_T \bar{\mathbf{A}}_\ell \frac{\partial \mathbf{U}^h}{\partial x_\ell}} \\ &= \sum_T \oint_{\partial\Omega_T} \mathbf{F}_\ell^h n_\ell \, d\Gamma\end{aligned}$$

and the contributions of internal edges cancel out (telescoping property).

For the Euler equations, such a conservative linearisation is obtained by a multidimensional extension of Roe's linearisation[36]. Indeed, assuming that Roe's parameter vector[3] $\mathbf{Z}$ is the unknown having linear variation on T, one exploits the property that both the vector of conserved variables $\mathbf{U}$ and the fluxes $\mathbf{F}_\ell$ are homogeneous functions of degree 2 in the components of $\mathbf{Z}$,

$$\begin{aligned}\int_{\Omega_T} \frac{\partial \mathbf{F}_\ell^h}{\partial x_\ell} d\Omega &\equiv \int_{\Omega_T} \frac{\partial \mathbf{F}_\ell}{\partial \mathbf{Z}}(\mathbf{Z}^h)\frac{\partial \mathbf{Z}^h}{\partial x_\ell} d\Omega \\ &\equiv \frac{\partial \mathbf{F}_\ell}{\partial \mathbf{Z}}(\bar{\mathbf{Z}})\frac{\partial \mathbf{Z}^h}{\partial x_\ell}\Omega_T \\ &\equiv \mathbf{A}_\ell(\bar{\mathbf{Z}}) \underbrace{\frac{\partial \mathbf{U}}{\partial \mathbf{Z}}(\bar{\mathbf{Z}})\frac{\partial \mathbf{Z}^h}{\partial x_\ell}\Omega_T}_{=\Omega_T \frac{\partial \mathbf{U}^h}{\partial x_\ell}}\end{aligned}$$

where $\bar{\mathbf{Z}} = \frac{1}{d+1}\sum_{\text{vertices}} \mathbf{Z}_i$ is the proper average state to ensure conservation.

Finding a conservative linearisation for more complex systems like the ideal MHD equations turns out to be difficult. However, work is going on to relax the necessity of finding a conservative linearisation: in reference[37], non-conservative residual distribution discretisations for general conservation laws are studied, which retain the correct weak solution behaviour in the limit of mesh refinement whenever a sufficient order of numerical quadrature is used.

System schemes

Similar to the scalar case, the cell residual is computed from eq. (38), giving

$$\Phi^T = \sum_i \mathbf{K}_i \mathbf{U}_i, \tag{40}$$

where $\mathbf{K}_i$ is now an inflow matrix defined as

$$\mathbf{K}_i = \frac{1}{d}\,\bar{\mathbf{A}}_\ell n_{i,\ell}, \tag{41}$$

The inflow matrices can also be written as

$$\mathbf{K}_i = \mathbf{L}_i^{-1}\Lambda_i \mathbf{L}_i \tag{42}$$

where the rows of $\mathbf{L}_i$ contain the left eigenvectors and the columns of $\mathbf{L}_i^{-1}$ the right eigenvectors and where Λ_i is a diagonal matrix of the eigenvalues. For introducing upwinding in the scheme use is made of matrices $\mathbf{K}_i^+$ and $\mathbf{K}_i^-$ defined by

$$\mathbf{K}_i^+ = \mathbf{L}_i^{-1}\Lambda_i^+ \mathbf{L}_i \qquad \mathbf{K}_i^- = \mathbf{L}_i^{-1}\Lambda_i^- \mathbf{L}_i \tag{43}$$

where Λ_i^+ contains the positive and Λ_i^- the negative eigenvalues of $\mathbf{K}_i$.

The design criteria for distribution matrices are similar as for distribution coefficients for the scalar advection equation, i.e.

$\mathcal{U}$**:** Upwind character. $\beta_i^T = 0$ when all eigenvalues of $\mathbf{K}_i$ (which are known to be real due to the hyperbolic nature of the system), are negative.

$\mathcal{P}$**:** Positivity. With $\Phi_i^T = \beta_i^T \Phi^T = \sum_j \mathbf{C}_{ij}\mathbf{U}_j$, the positivity condition becomes $\mathbf{C}_{ij} \le 0 \quad \forall j \ne i$. This definition is connected to a previous work by Lax and Liu[38], itself related to a result by P.D. Lax (see[39], page 120), on the L^2 stability of symmetric hyperbolic systems. In practice it is difficult to handle this condition, so that it may be useful to consider another condition relying on entropy considerations[24]. The idea is to look at system (36) as $d+2$ conservation equations endowed with an entropy inequality

$$\frac{\partial s}{\partial t} + \vec{u}\cdot\vec{\nabla} s \ge 0$$

or

$$\frac{\partial (\rho s)}{\partial t} + \frac{\partial \rho s u_\ell}{\partial x_\ell} \ge 0.$$

The second law of thermodynamics, and following Tadmor[40], states that the entropy of a fluid particle increase in time. Mathematically speaking, the specific entropy s is a *concave* function of $\tau = \frac{1}{\rho}$ and the specific energy ε. Thanks to that, one can expect that τ and ε will remain bounded in time : this is a stability property. One tries to mimic this behavior by demanding that $\nabla s_i \cdot \Phi_i^T$, in other words, the (specific) entropy production of the scheme within the triangle T, for each vertex is bounded by terms like $\sum_j c_{ij}(s_i - s_j)$ with $c_{ij} \ge 0$: this is an approximation of the transport term $\vec{u}\cdot\vec{\nabla} s$.

$\mathcal{LP}$**:** Linearity preservation. Second order accuracy at steady state is obtained if the distribution matrices β_i^T remain bounded as $\Phi^T \to 0$. As previously mentioned, a relaxed version of this property[24] is quite interesting for systems since it avoids to define explicitly the distribution matrices β_i^T : the computation is generally difficult, and it is an ill posed problem since in dimension d, there are $(d+2)\times(d+2)$ unknowns for $d+2$ equations to solve.

The relaxed version of this property is expressed, for a *regular mesh* and for a *regular* solution of the PDE system (36), by

$$\Phi_i^T = O(h^3). \qquad (44)$$

If $\Phi_i^T = \beta_i^T \Phi^T$ with β_i^T uniformly bounded as the mesh size $h \longrightarrow 0$, the residuals satisfy (44) because $\Phi^T = O(h^3)$. This is a consequence of two distinct facts :

- The piecewise linear interpolant Z^h of the regular function Z satisfies $||Z^h - Z|| = O(h^2)$ for the L^2 norm.
- One has, for *steady problems*

$$\begin{aligned}
\int_{\Omega_T} \vec{\nabla} \cdot \vec{\mathbf{F}}(U^h) &= \int_{\Omega_T} \left(\vec{\nabla} \cdot \vec{\mathbf{F}}(U^h) - \vec{\nabla} \cdot \vec{\mathbf{F}}(U)\right) d\Omega \\
&= \int_{\partial\Omega_T} \left(\vec{\mathbf{F}}(U^h) - \vec{\mathbf{F}}(U)\right) d\Gamma \\
&= O(h^3)
\end{aligned}$$

The first equality comes from the fact that U is a steady solution, the last one comes from (a) $||Z^h - Z|| = O(h^2)$, (b) $\mathbf{F}$ is Lipschitz continuous w.r.t Z, (c) the length of boundary $\partial\Omega_T$ is $O(h)$.

$\mathcal{I}$: Invariance for similarity transformations. This property means that the residual sent to the nodes in conservative variables $\mathbf{U}$ is independent of the choice of variables in which the actual distribution is performed. Consider a set of characteristic variables $\mathbf{W}$, defined by the similarity tranformation $\partial \mathbf{W} = \frac{\partial W}{\partial x_U} \partial \mathbf{U}$. The scheme is invariant for this transformation if the distribution matrices for the different sets of variables satisfy[41] : $\beta_i^U = \frac{\partial U}{\partial x_W} \beta_i^W \frac{\partial W}{\partial x_U}$.

Many of the schemes listed in Table 1 can be formally extended to systems[41].

N-scheme

The system-N scheme is defined by

$$\Phi_i^{T,N} = \mathbf{K}_i^+ (\sum_j \mathbf{K}_j^-)^{-1} \sum_j \mathbf{K}_j^- (\mathbf{U}_i - \mathbf{U}_j) \qquad (45)$$

In[42] two important properties of the system N-scheme are shown for symetrizable systems like the Euler equations :

1. The scheme is always well defined and depends continuously on the parameter. The problem comes from the matrix $\sum_j \mathbf{K}_j^-$ which can become singular. For the Euler equations, the singularity points correspond to stagnation points. If $\sum_j \mathbf{K}_j^-$ may be singular, however, for any j, the matrix $(\sum_j \mathbf{K}_j^-)^{-1} K_j^-$ is always defined, and depends continuously of the data. The key arguments are (a) the Jacobian matrices have only one common eigenvector which corresponds to the entropy transport, (b) the other eigenvectors belong to an orthorgonal vector space which does not depend on $n_{i,\ell}$.
2. The system N–scheme is dissipative. More precisely, setting $\mathbf{V}_i = \nabla(\rho s)_i$, the entropy production of the system N–scheme, $\sum_i \mathbf{V}_i \cdot \Phi_i^N$ on T can be written as

$$\sum_T \mathbf{V}_j \cdot \Phi_j^N = \frac{1}{2} \sum_T \mathbf{V}_j^t \mathbf{K}_j \mathbf{V}_j + \mathcal{Q}^N(\mathbf{V}_i, \mathbf{V}_j, \mathbf{V}_k)$$

where $\mathcal{Q}^N$ is a negative quadratic form. The term $\frac{1}{2} \sum_T \mathbf{V}_j^t \mathbf{K}_j \mathbf{V}_j$ is a consistent approximation of $\int_{\Omega_T} \frac{\partial(\rho s u_\ell)}{\partial x_\ell} d\Omega$.

LDA-scheme

The system-LDA scheme is defined by

$$\beta_i^{T,LDA} = \mathbf{K}_i^+ (\sum_j \mathbf{K}_j^+)^{-1} \qquad (46)$$

The same arguments as above indicate that the distribution matrix β_i is always defined whatever the flow. No dissipation property of the scheme has yet been proven. The entropy production of the system–LDA scheme has also the form

$$\sum_T \mathbf{V}_j \cdot \Phi_j^{LDA} = \frac{1}{2} \sum_T \mathbf{V}_j^t \mathbf{K}_j \mathbf{V}_j + \mathcal{Q}^{LDA}(\mathbf{V}_i, \mathbf{V}_j, \mathbf{V}_k),$$

but the quadratic form $\mathcal{Q}^{LDA}$ is neither positive nor negative. However, numerical experiments seem to indicate the dissipativity properties of the scheme, but the analysis is certainly less local as for the system–N scheme. In[24] the following property is shown for symmetric systems,

$$\mathcal{Q}^{LDA} \leq \mathcal{Q}^N,$$

the system–LDA scheme is less dissipative than the system–N scheme.

System PSI scheme

The non-linear PSI scheme proves to be more difficult to generalize. Considering the scalar PSI scheme as a limited N-scheme, its formal generalisation to systems is

$$\beta_i^{T,PSI} = \left(\sum_j \beta_j^{T,N^+} \right)^{-1} \beta_i^{T,N^+} \qquad (47)$$

However, the distribution matrix of the N-scheme $\beta_i^{T,N}$ is not explicitly defined by eq. (45). For diagonalisable systems, the condition of invariance under similarity transformations suffices to define $\beta_i^{T,N}$ and hence $\beta_i^{T,PSI}$ uniquely. For general non-commuting systems, the invariance condition is no longer sufficient. The system PSI scheme used in the numerical applications is based on one particular definition of $\beta_i^{T,N}$ which satisfies this condition. Further details are given in[10].

Non-linear monotone blending scheme

The construction of non-linear positive and linearity preserving schemes for systems is still an ongoing research topic. New developments, based on the reinterpretation of the scalar PSI scheme as a blended N/LDA scheme are discussed in[28].

The construction relies on the study of the entropy production within one cell. One first assumes that the system–N scheme satisfies an equality of the form

$$\nabla s_i \cdot \Phi_i^N \leq \sum_j c_{ij}(s_i - s_j)$$

with $c_{ij} \geq 0$. The second step is to consider the blended scheme $\Phi_i = \mathbf{l}\Phi_i^N + (\mathbf{Id} - \mathbf{l})\Phi_i^{LDA}$ where l is a $(d+2)\times(d+2)$ matrix. The conservation is obtained *a priori* since $\sum_T \Phi_i^N = \sum_T \Phi_i^{LDA}$.

Then we compute the entropy production at each vertex of T

$$\nabla s_i \cdot \Phi_i = \frac{\nabla s_i \cdot \Phi_i}{\nabla s_i \cdot \Phi_i^N}\ \nabla s_i \cdot \Phi_i^N$$

and the positivity condition is ensured provided that

$$\frac{\nabla s_i \cdot \Phi_i}{\nabla s_i \cdot \Phi_i^N} \geq 0$$

for each vertex of T.

The simpliest matrix limiter function is $\mathbf{l} = l\mathbf{Id}$ where l is a real number. Setting $r_i = \dfrac{\vec{\nabla} s_i \cdot \Phi_i^{LDA}}{\vec{\nabla} s_i \cdot \Phi_i^N}$, a solution is given by

$$l = \max_T\left(\varphi\left(r_i\right)\right).$$

More complex constructions using the eigen–structure of the system can be found in[24].

Entropy fix

The residual distribution schemes are genuine multidimensional extensions of Roe's scheme. Therefore, they still have in common some failings with Roe's scheme. Because shocks can be captured over a single cell, unphysical expansion shocks may occur, which are entropy violating numerical solutions. Also in common with many flux difference schemes, they may for very regular or sufficiently refined grids produce carbuncle phenomena when trying to compute strong bow shocks. A multidimensional entropy fix and a carbuncle cure for the residual distribution schemes have been developed recently and will be discussed in a forthcoming paper[43].

The removal of an expansion shock is illustrated for a steady Mach 3 Euler flow over a forward facing step. The testcase is the steady state limit of the unsteady testcase proposed by Colella[44] and discussed further in the paper. Also the mesh is the same. Figure 6a shows the solution computed with the second order blended scheme on a grid with 17300 nodes. An expansion shock is seen to emanate from the corner over which the flow normally expands gradually. Figure 6b shows that with the entropy fix the expansion shock is completely removed.

Transformations and preconditioning

The matrix distribution schemes presented above are invariant under a similarity transformation. It is nevertheless useful to apply a similarity transformation to the linearized hyperbolic system in order to achieve maximum decoupling for the following reasons. On one hand, this reduces the computational cost thanks to the considerable simplification of the distribution expressions and on the other hand, this allows to select *different* distribution schemes on the various decoupled systems/scalar equations. Specifically, with the similarity transformation $\partial\mathbf{U} = T\partial\mathbf{Q}$, the discrete equations (37) are rewritten as

$$\mathbf{R}_i = \sum_T T^T \beta_{Q\,i}^T \Phi_Q^T = 0 \tag{48}$$

where $\Phi_Q^T = \sum_i \mathbf{K}_{Q\,i}\mathbf{Q}_i$. Partial decoupling can be achieved if the flux jacobians $\mathbf{A}_\ell$ have some eigenvectors in common. For the Euler equations, the flux jacobians $\mathbf{A}_\ell$ have one common eigenvector, so that it is possible to decouple one scalar equation from the original system, leaving a coupled 3×3 system and one decoupled scalar equation in 2D. The transformation to symmetrizing variables defined as $\partial\mathbf{Q} = (\frac{\partial p}{\rho a}, \partial\mathbf{u}, \partial p - a^2\partial\rho)^t$ accomplishes this task. The decoupled scalar equation is nothing else than the entropy advection equation, which is well known to derive from the Euler equations.

As shown in[10], additional decoupling may be achieved by preconditioning, namely the system of equations is rewritten as (the original conservative variables are used here, but the same procedure is done in practice for the symmetrizing variables)

$$\mathbf{P}^{-1}\left[\mathbf{PA}\frac{\partial\mathbf{U}}{\partial x} + \mathbf{PB}\frac{\partial\mathbf{U}}{\partial y}\right] = 0 \tag{49}$$

and the residual distribution method is applied to the preconditioned system between brackets. The optimal preconditioning was found to be the van Leer-Lee-Roe preconditioning[45], which allows to decouple one additional equation, namely the advection equation for the total enthalpy.

Viscous terms

For the Navier-Stokes equations, the viscous terms are discretised using the finite element interpretation

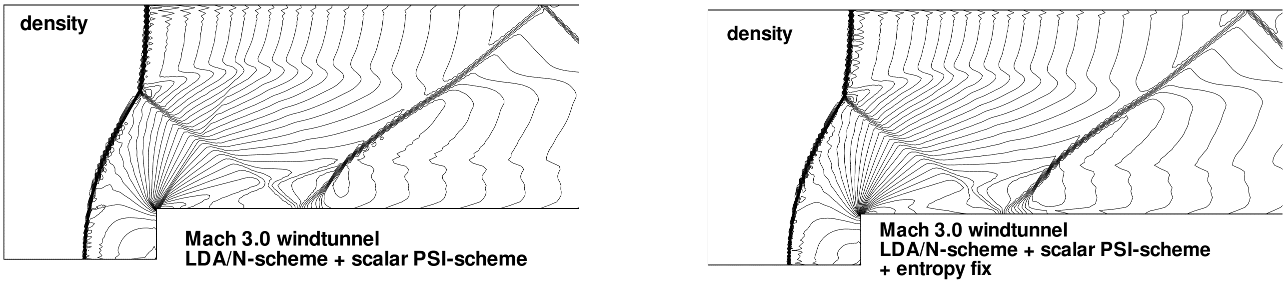

a) Blended scheme. **b) Blended scheme with entropy fix.**

Fig. 6 Steady Euler flow in a channel with a forward facing step (density contours).

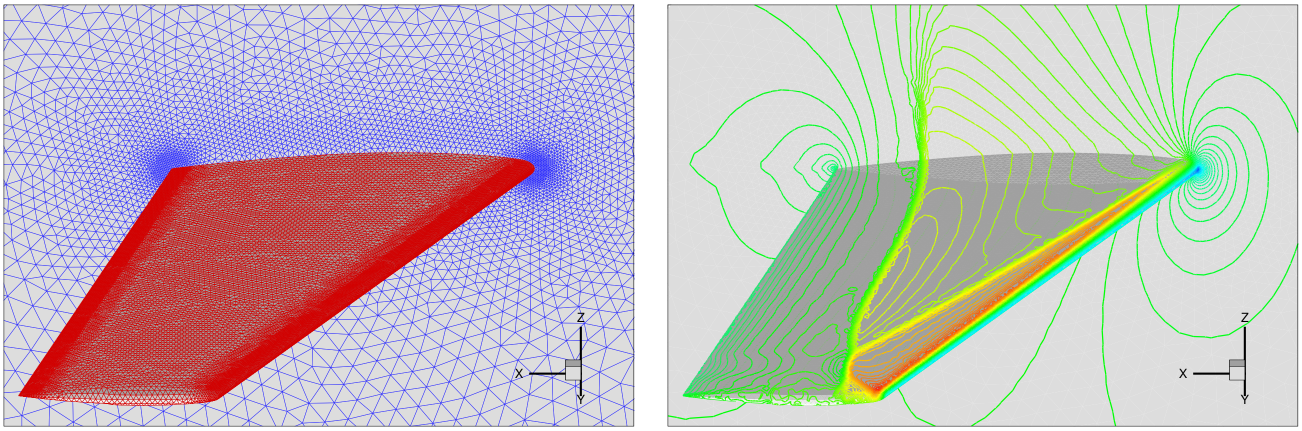

a) Surface grid. **b) Mach number isolines with second order blended scheme.**

Fig. 7 Transonic flow over ONERA M6 wing ($M_\infty = 0.84$, $\alpha = 3.06°$).

of the schemes presented before. Specifically, the space discretisation of the divergence of the stress tensor $\nabla \cdot \bar{\bar{\tau}}$ is

$$\sum_T \int_T \omega_i^T \nabla \cdot \bar{\bar{\tau}} \, d\Omega = \sum_T \int_{\partial T} \omega_i^T \bar{\bar{\tau}} \cdot \vec{n} d\Gamma - \sum_T \int_T \nabla \omega_i^T \cdot \bar{\bar{\tau}} \, d\Omega.$$

Now, since ω_i^T differs from the P1 shape function φ_i only by a piecewise constant, $\nabla \omega_i^T = \nabla \varphi_i$, so that, for interior points, the discretisation reduces to a Galerkin finite element discretisation.

Applications in steady flow

Capabilities of upwind residual distribution schemes are now illustrated by a couple of computational examples.

Inviscid transonic flow over the M6 wing

The ONERA M6 wing is a widely used testcase for three-dimensional flows from subsonic to transonic speeds[46]. The selected transonic case is $M_\infty = 0.84$, $\alpha = 3.06°$. The grid consists of 316275 nodes and 1940182 tetrahedra. The far-field boundary is half a sphere with a radius of 12.5 root-chord lengths. The computation of this testcase with the present multidimensional upwind method employed the van Leer-Lee-Roe preconditioning, allowing a hybrid discretisation. The decoupled advection equations for entropy and total enthalpy are discretised with the scalar PSI-scheme, while the acoustic subsystem is discretised with a blended system LDA/N-scheme. To give an indication of how the multidimensional upwind method performs compared to standard finite volume methods, the same testcase has also been computed with the Jameson-Schmidt-Turkel (JST) artificial dissipation scheme, a matrix dissipation (MATD) scheme and the Roe upwind scheme with Venkatakrishnan's reconstruction. A plot of the grid and Mach number isolines on the symmetry plane and the surface of the wing are shown in Fig. 7.

Plots for the pressure coefficient C_p and the relative total pressure loss, defined as $1 - p_t/p_{t\infty}$, in the 80% span cross-section are shown in Fig. 8. From these figures it is clear that the multidimensional upwind method is much less dissipative in the leading edge region and that it has a better shock capturing.

Inviscid transonic flow over a complete aircraft

To demonstrate the applicability of the present multidimensional upwind method to a complete aircraft configuration, the transonic flow over a generic model of the Falcon 2000 executive jet has been computed.

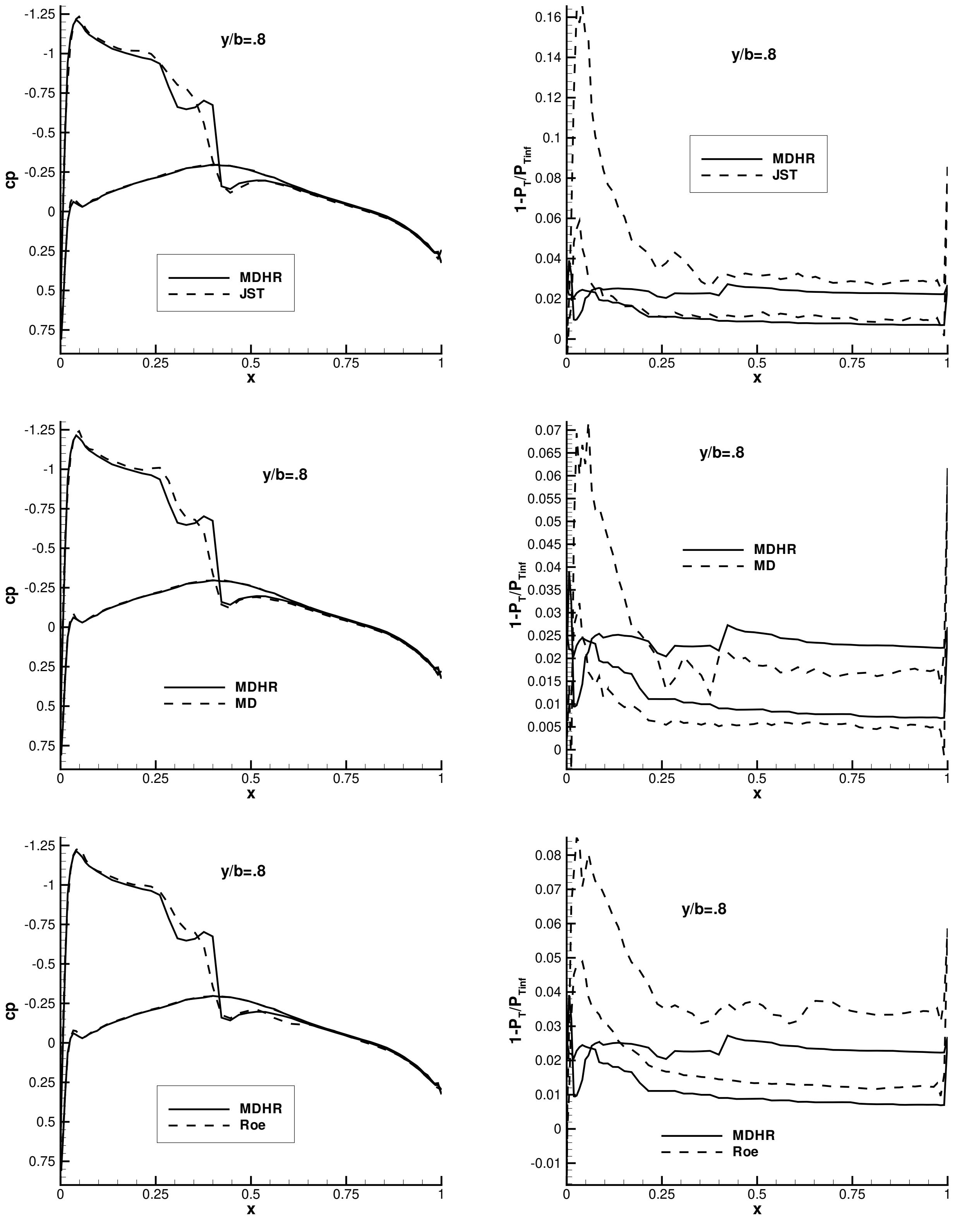

Fig. 8 ONERA M6 wing: C_p and total pressure loss distributions at 80% span, upwind residual distribution schemes versus finite volume schemes.

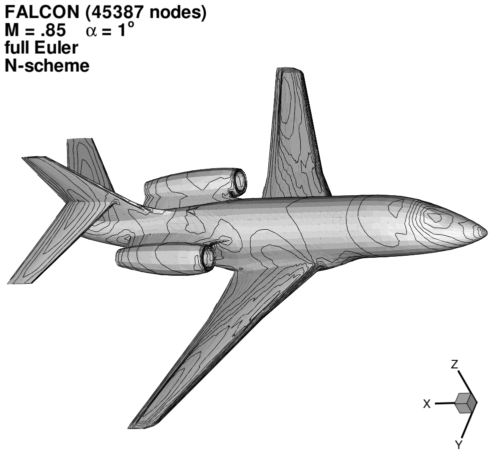

a) N-scheme, Mach number contours.

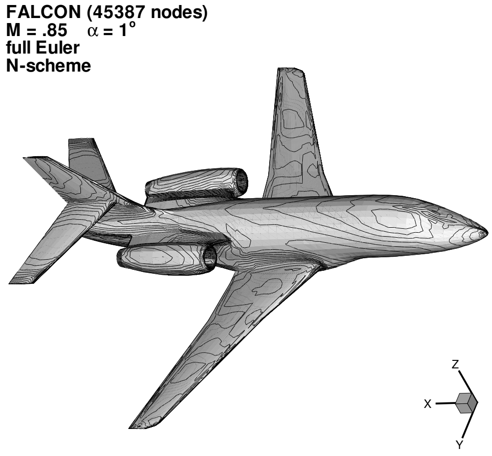

b) N-scheme, entropy contours.

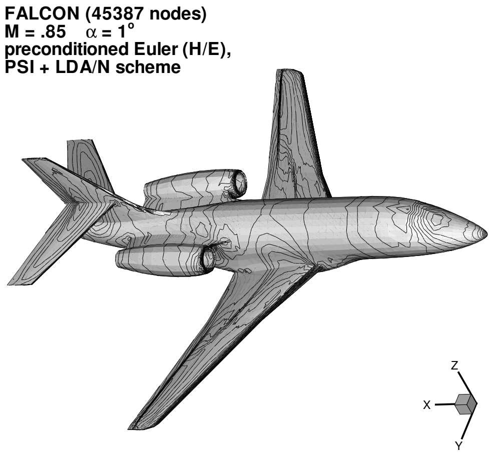

c) LDA/N blended scheme, Mach contours.

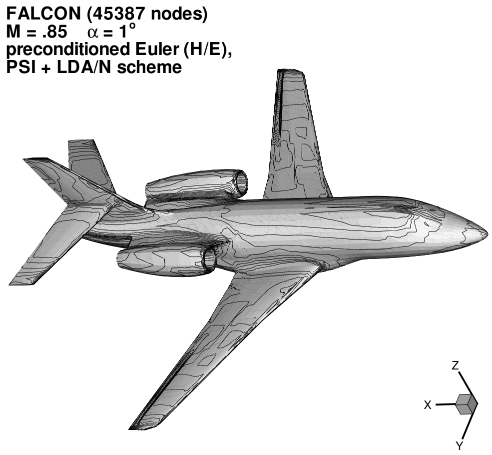

d) LDA/N blended scheme, entropy contours.

Fig. 9 Falcon 2000, inviscid transonic flow at $M_\infty = 0.85$, $\alpha = 1.0°$, half-model mesh with 45387 nodes.

The grid for a half model consists of 45387 nodes and 255944 tetrahedra. The selected testcase corresponding to cruise conditions is $M_\infty = 0.85, \alpha = 1.0°$. The solutions computed with monotone first and second-order multidimensional upwind schemes are compared. For the first order computation the system N-scheme is applied directly to the full Euler equations. The second order computation employs the van Leer-Lee-Roe preconditioning, where the advection equations for entropy and total enthalpy are discretised with the scalar PSI-scheme and the acoustic subsystem is discretised with the blended system LDA/N-scheme. Figure 9 compares the Mach number and entropy isolines for these two solutions. The better shock capturing and lower spurious entropy generation in the leading edge region of the wing and the engine pylon are clearly observed for the second order scheme.

Transonic turbulent channel: Délery's experiment C

This testcase of a transonic shock boundary layer interaction was experimentally investigated in the early eighties by Délery[47]. It serves to illustrate the capabilities of the present method in computing high Reynolds number turbulent flow. The subsonic inlet boundary conditions are $T_t = 300K$, $P_t = 96kPa$ and $\alpha = 0°$, while at the outlet a pressure of 61.5 kPa has been prescribed. Furthermore a zero thickness boundary layer is assumed at inlet. A hybrid grid is used for this computation, obtained by combining hyperbolic structured grids in the boundary layer with frontal Delaunay generated isotropic grids in the mean flow[48]. The grid is shown in figure 10. It consists of 10420 nodes and 20466 triangular elements and is refined in the region of interest.

The initial normal spacing near the wall at the inlet is 1.0×10^{-6} and at the outlet 5.7×10^{-6}. Mach number isolines of the second order scheme in combination with the two-equation SST model of Menter[49], are given in figure 11. The lambda-shock, which linear $k - \varepsilon$ and $k - \omega$ models fail to predict, is clearly visible. Wall pressure distributions, made dimensionless by the total pressure of 96.0 kPa, are compared with experiments in the figures 12 and 13.

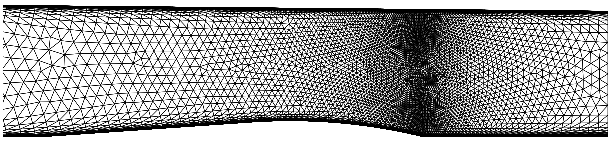

Fig. 10 Grid for Délery's test case C: 10420 nodes, 20466 elements.

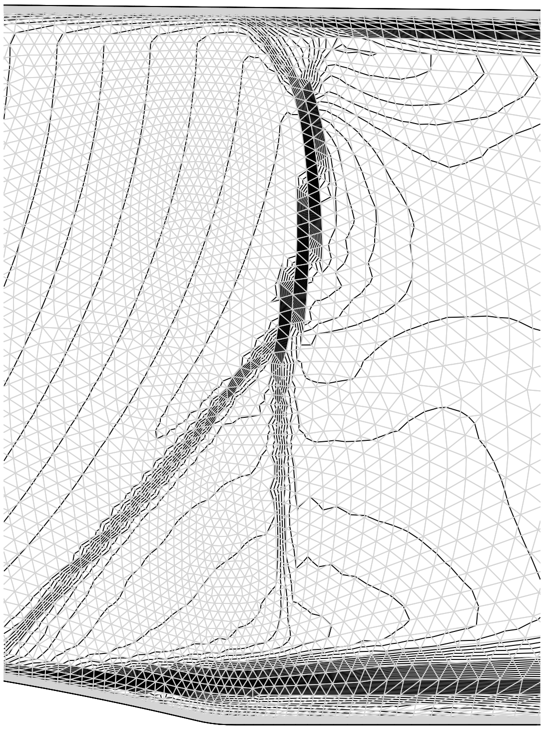

Fig. 11 Mach number isolines superposed on the mesh, in the interaction region for the Délery test case C: min = 0.0, max = 1.40, step = 0.025.

It can be seen that upstream of the shock the computed pressure distributions perfectly match the experimental data, which is logical, for these distributions are determined by inviscid phenomena. However, after the shock all computations are quite far off from the experimental data, although the SST and Spalart-Allmaras models are significantly better than the $k-\omega$ model.

Applications in Unsteady flow

In the present Section the above discussed algorithms for time accurate simulation are applied to the Euler equations for inviscid flow. The test problem is the flow over a forward facing step, which is injected in a uniform Mach 3 flow at $t = 0$[44]. The inflow conditions are $\rho = 1.4$, $p = 1$, $u = 3$ and $v = 0$. We take $\gamma = 1.4$. Density contours are shown at $t = 1$ and $t = 3$. The top panels of figure 15 give the reference solution[44] obtained with a PPM finite volume scheme on a grid with 15200 cells. The middle and lower panels

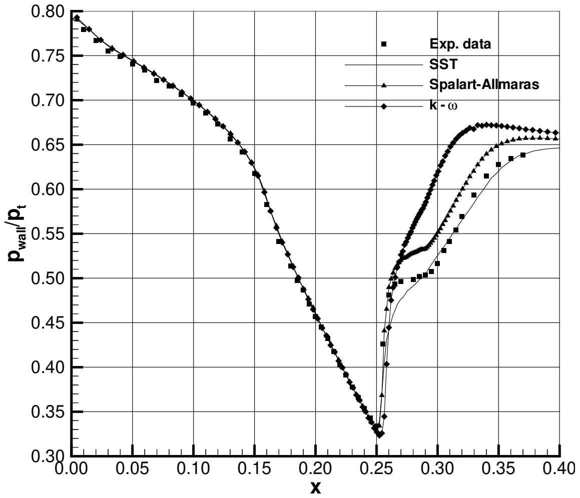

Fig. 12 Experimental and computed pressure distribution on the lower wall.

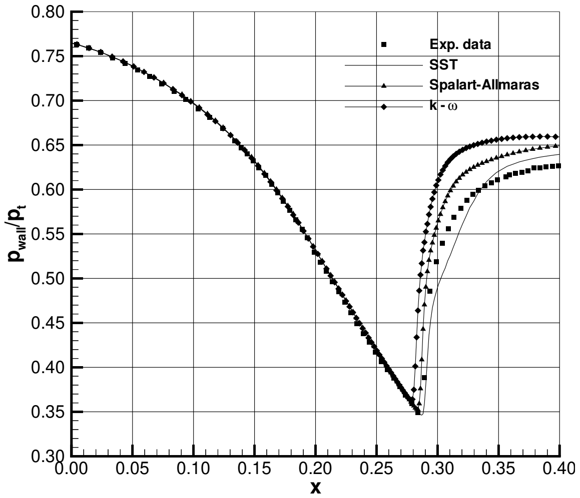

Fig. 13 Experimental and computed pressure distribution on the upper wall.

give the results of simulation with the residual distribution schemes on a grid with 17320 nodes and 33998 cells (figure 14). The middle panels represent the solution obtained by Ferrante[32] using the FCT procedure with the implicit consistent LDA scheme as high order scheme, and the explicit N scheme without mass matrix as low order scheme. The time step is thus

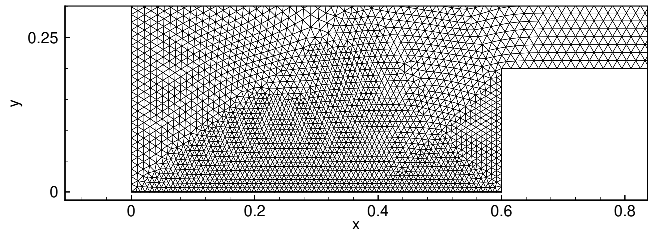

Fig. 14 Detail of the computational grid for the channel flow with step.

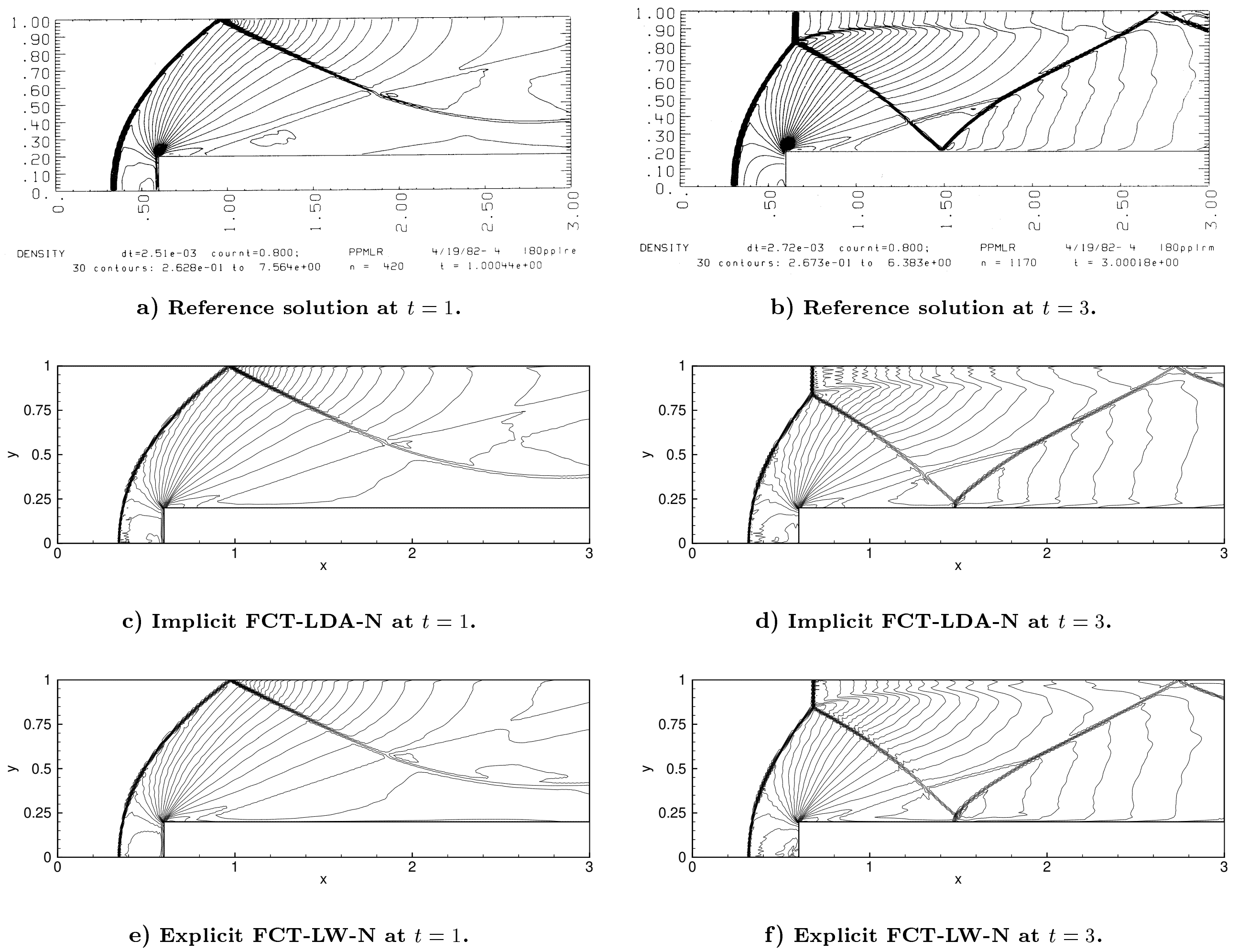

a) **Reference solution at $t = 1$.**

b) **Reference solution at $t = 3$.**

c) **Implicit FCT-LDA-N at $t = 1$.**

d) **Implicit FCT-LDA-N at $t = 3$.**

e) **Explicit FCT-LW-N at $t = 1$.**

f) **Explicit FCT-LW-N at $t = 3$.**

Fig. 15 Euler flow in a channel with a forward facing step (density contours).

restricted by a CFL condition. The cell-wise limiting factor is obtained by taking the minimum of the limiting factors calculated for the density and the energy. The bottom panels are obtained using FCT with explicit LW as high order scheme, and explicit N as low order scheme, both without mass matrix[35]. For these FCT-LW-N simulations the limiting is performed on the density and the two momentum components. In the middle and bottom panels 30 density contours are equally spaced between 0.1 and 8.1.

Figures 6 and 15 indicate that the results obtained by using the FCT procedure generally give consistent results with sharp shocks and without large oscillations. For $t = 3$ (figure 15) small oscillations can be observed in the FCT results, especially in the corner region before the step, following the Mach stem at the upper boundary for the FCT-LDA-N scheme, and following the second shock for the FCT-LW-N scheme. The implicit FCT-LDA-N and the explicit FCT-LW-N schemes give quite similar results, but the FCT-LDA-N solution shows stronger oscillations following the Mach stem. It has to be noted that the FCT procedure is not very robust. For instance, for the FCT-LW-N scheme, using the traditional limiting variables density and energy[32, 50] lead to failure of the scheme, while a solution could be obtained by choosing the density and momentum components for the limiting. It can thus be concluded that the residual distribution FCT procedure gives satisfactory results for this time dependent flow with strong shocks, although small oscillations, robustness, and a high computational cost remain points of concern.

Conclusion

Residual distribution schemes have reached a certain degree of maturity for the solution of the steady compressible flow equations on unstructured grids composed of triangles or tetrahedra. From the theoretical point they combine the compactness of the Finite Element stencil with the shock capturing properties of Roe-type Finite Volume schemes. Applications have been shown to complex aerodynamical flows, both in the subsonic, transonic and supersonic regime, which demonstrate the excellent shock capturing properties and accuracy. Nevertheless, it is clear that the full potential of the approach has not been exploited yet, and more work is still required on the theoretical side to improve robustness and efficiency for systems, even for steady state computations. A promising development in this respect is the development of new blending schemes for systems, which in the scalar case boil down to the well established optimal scalar schemes.

Extensions to unsteady flow equations have started. Preliminar results have been obtained using an explicit Lax-Wendroff or an implicit consistent mass matrix approach, but an FCT procedure had to be used to recover monotonicity. A much more promising way is the development of new space-time residual distribution schemes as described in this paper.

Application to more complex systems like the ideal MHD equations, or the equations for two-phase flow, has not been dicussed in this survey, but also in this area work is underway and promising results have been obtained[51].

Acknowledgements

This paper summarises over 10 years of research at VKI and INRIA and the UNIVERSITY OF BORDEAUX. At VKI the research was carried out in collaboration with our colleague G. Degrez and with a series of Ph.D. candidates and Diploma Course members: R. Struijs, H. Paillère, A. Bonfiglioli, E. van der Weide, J.-C. Carette, E. Issman, N. Waterson, S. Bogaerts, A. Csik, H. De Sterck, A. Ferrante, M. Ricchiuto. At INRIA and the University of Bordeaux, the research was carried out with our colleagues K. Mer–Nkonga, B. Nkonga and M. Mezine. The contributions by P.L. Roe (University of Michigan), T. J. Barth (NASA Ames Research Center), M. Rudgyard (University of Warwick, UK) and D. Sidilkover (ICASE) during this long period make this work a truely trans-atlantic effort. The ONERA M6 wing and the generic Falcon computations were carried out within the collaborative IMT project IDeMAS funded by the European Commission. The reference computations of the ONERA M6 test case were performed by E. van der Weide at Daimler-Chrysler Aerospace. The grid for the generic Falcon configuration was provided by Dassault Aviation.

References

[1] A. Jameson, W. Schmidt, and E. Turkel. Numerical solutions of the Euler equations by finite-volume methods using Runge-Kutta time-stepping. AIAA Paper 81-1259.

[2] S. K. Godunov. A finite difference method for numerical computation of discontinuous solutions of the equations of fluid dynamics. *Mat.Sb.*, 47:271–306, 1959.

[3] P. L. Roe. Approximate Riemann solvers, parameter vectors and difference schemes. *Journal of computational physics*, 43:357–352, 1981.

[4] B. van Leer. Flux-vector splitting for the Euler equations. *Lecture Notes in Physics*, 170:507–512, 1982.

[5] S. P. Spekreijse. *Multigrid solution of the steady Euler equations.* PhD thesis, T. U. Delft, 1987.

[6] A. Jameson. Artificial diffusion, upwind biasing, limiters and their effect on accuracy and multigrid convergence in transonic and hypersonic flows. AIAA Paper 93-3359.

[7] B. Cockburn. Discontinuous Galerkin methods for convection-dominated problems. In T.J. Barth and H. Deconinck, editors, *High-order methods for computational physics*, volume 9 of *Lecture Notes in Computational Science and Engineering.* Springer, 1999.

[8] A. N. Brooks and T. J. R. Hughes. Streamline upwind/Petrov-Galerkin formulations for convection dominated flows with particular emphasis on the incompressible Navier-Stokes equations. *Comp. Meth. Mech. Eng.*, 32:199–259, 1982.

[9] T. De Mulder. Stabilized finite element methods for incompressible flows. VKI LS 1997-02, 1997.

[10] H. Paillère, H. Deconinck, and E. van der Weide. Upwind residual distribution methods for compressible flow: an alternative to finite volume and finite element methods. VKI LS 1997-02, 1997.

[11] J. Rice and R. Schnipke. A monotone streamline upwind method for convection-dominated problems. *Computer Methods in Applied Mechanics and Engineering*, 48:313–327, 1985.

[12] G.D. Raithby. Skew upstream differencing schemes for problems involving fluid flow. *Computer Methods in Applied Mechanics and Engineering*, 9:153–164, 1976.

[13] K.G. Powell, B. van Leer, and P.L. Roe. Towards a genuinely multi-dimensional upwind scheme. In *VKI LS 1990-03, Computational Fluid Dynamics*, 1993.

[14] I.H. Parpia and D.J. Michalec. Grid-independent upwind scheme for multidimensional flow. *AIAA Journal*, 31(4):646–651, 1993.

[15] P. Van Ransbeeck and C. Hirsch. *Multidimensional upwind schemes for the Euler/Navier-Stokes equations on structured grids*, volume 57 of *Notes on Numerical Fluid Mechanics*, pages 305–338. Vieweg Verlag, 1996.

[16] R.-H. Ni. A Multiple Grid Scheme for Solving the Euler Equations. *AIAA Journal*, 20:1565–1571, 1981.

[17] M. Rudgyard. Cell-vertex methods for steady inviscid flow. In *VKI LS 1993-04, Computational Fluid Dynamics*, 1993.

[18] P. L. Roe. Fluctuations and signals, a framework for numerical evolution problems. In K. W. Morton & M. J. Baines, editor, *Numerical Methods for Fluid Dynamics*, pages 219–257. Academic Press, 1982.

[19] P. L. Roe. Linear advection schemes on triangular meshes. CoA Report 8720, Cranfield Inst. of Tech., 1987.

[20] E. Issman, G. Degrez, and H. Deconinck. Implicit upwind residual-distribution Euler and Navier-Stokes solver on unstructured meshes. *AIAA Journal*, 34(10):2021–2029, 1996.

[21] E. Issman and G. Degrez. Non-overlapping preconditioners for a parallel implicit Navier-Stokes solver. *Future Generation Computer Systems*, 13:303–313, 1997/1998.

[22] E. van der Weide, H. Deconinck, E. Issman, and G. Degrez. A parallel, implicit, multidimensional upwind residual distribution method for the Navier-Stokes equations on unstructured grids. *Computational Mechanics*, 23(2):199–208, 1999.

[23] R. Abgrall and K. Mer. Un théorème de type lax–wendroff pour les schémas distributifs. Technical Report 98010, Mathématiques Appliquées de Bordeaux, 1998.

[24] R. Abgrall. Toward the ultimate conservative scheme : Following the quest. *JCP*, accepted for publication.

[25] H. Paillère and H. Deconinck. *Compact cell vertex convection schemes on unstructured meshes*, volume 57 of *Notes on Numerical Fluid Mechanics*, pages 1–49. Vieweg Verlag, 1996.

[26] D. Sidilkover. A genuinely multidimensional upwind scheme and efficient multigrid solver for the compressible Euler equations. Technical Report 94-84, ICASE, 1994.

[27] D. Sidilkover and P.L. Roe. Unification of some advection schemes in two dimensions. Technical Report 95-10, ICASE, 1995.

[28] R. Abgrall. Construction of genuinely multidimensional upwind schemes. 2nd International Symposium on Finite Volumes for Complex Applications, July 1999.

[29] R. Abgrall. Toward the ultimate conservative scheme : Following the quest. *J. Comput. Phys.*, 2000. *to appear.*

[30] T. De Mulder. *Stabilized finite element methods for turbulent incompressible single-phase and dispersed two-phase flows.* PhD thesis, K. U. Leuven, Leuven, Belgium, 1997.

[31] J. Maerz. Improving time accuracy for residual distribution schemes. VKI Project Report 1996-17, 1976.

[32] A. Ferrante. Solution of the unsteady euler equations using residual distribution and flux corrected transport. VKI Project Report 1997, 1997.

[33] M.E. Hubbard and P.L. Roe. Compact high-resolution algorithms for time-dependent advection on unstructured grids. Preprint, 1999.

[34] J.P. Boris and D.L. Book. Flux corrected transport i.shasta, a transport algorithm that works. *Computational Physics*, 11, 1973.

[35] M. Ricchiuto. Time accurate solution of hyperbolic partial differential equations using fct and residual distribution. VKI Stagiaire Report 1999-33, 1999.

[36] H. Deconinck, P. L. Roe, and R. Struijs. A multidimensional generalization of Roe's flux difference splitter for the Euler equations. *Computers and Fluids*, 22:215–222, 1993.

[37] R. Abgrall and T. J Barth. Residual distribution schemes for conservation laws via adaptive quadrature. In *Schémas distribués en mécanique des fluides et applications, écoles CEA-EDF-INRIA*, 2000.

[38] P.D. Lax and X.-D. Liu. Solution of two-dimensional Riemann problems of gas dynamics by positive schemes. *SIAM Journal on Scientific Computing*, 19(2):319–340, 1998.

[39] R. D. Richtmeyer and K. W. Morton. *Difference methods for initial-value problems*. Interscience Tracts in Pure and Applied Mathematics. Interscience Publishers, 1967. second edition.

[40] E. Tadmor. The numerical viscosity of entropy stable schemes for systems of conservation laws. *Math. Comp.*, 49:91–103, 1987.

[41] E. van der Weide and H. Deconinck. Positive matrix distribution schemes for hyperbolic systems, with application to the Euler equations. In *Proceedings of the 3rd European CFD Conference*, pages 747–753, Paris, France, 1996. Wiley.

[42] R. Abgrall and T.J. Barth. Weighted residual distribution schemes for conservation laws via adaptive quadrature. *in preparation*, 2000.

[43] K. Sermeus and H. Deconinck. Entropy fix and shock fix for the residual distribution schemes. In *AIAA CFD Conference*, 2001. *in preparation.*

[44] P. Colella and P. Woodward. The numerical simulation of two-dimensional fluid flow with strong shocks. *J. Comput. Phys.*, 54:115–173, 1984.

[45] B. van Leer, W. T. Lee, and P. L. Roe. Characteristic time stepping or local preconditioning of the Euler equations. AIAA Paper 91-1552-CP.

[46] A Selection of Experimental Test Cases for the Validation of CFD codes. AGARD Advisory Report No 303, 1994.

[47] J.M. Délery. Experminental Investigation of Turbulence Properties in Transonic Shock/Boundary-Layer Interactions. *AIAA-Journal*, 21(2):180–185, 193.

[48] J.-C. Carette and H. Deconinck. Adaptive hybrid remeshing and SUPG/multiD-upwind solver for compressible high Reynolds number flows. AIAA Paper 97-1857-CP.

[49] F.R. Menter. Two-Equation Eddy-Viscosity Turbulence Models for Engineering Applications. *AIAA-Journal*, 32(8):1598–1605, 1994.

[50] R. Loehner, K. Morgan, J. Peraire, and M. Vahdati. Finite element flux-corrected transport (FEM-FCT) for the euler and navier-stokes equations. *Int. J. Numer. Meth. Fluids*, 7:1093–1109, 1987.

[51] H. Deconinck A. Csik and S. Poedts. Monotone residual distribution schemes for the ideal 2d magnetohydrodynamic equations on unstructured grids. AIAA Paper 99-3325.